Journal of Marine Science and Technology

Volume 1 | Issue 1 Article 10

Numerical Study of Spray Flame Characteristics

C.Y. Lin
Department of Marine Engineering and Technology National Taiwan Ocean University Keelung, Taiwan, R.O.C.

Journal of Marine Science and Technology. Vol. 1, No. 1, pp. 65-71 (1993)

NUMERICAL STUDY OF SPRAY FLAME CHARACTERISTICS

C.Y. Lin

Department of Marine Engineering and Technology
National Taiwan Ocean University
Keelung, Taiwan, R.O.C.

Key words: spray combustion, air-atomized, turbulence model.

ABSTRACT

A numerical method was considered to calculate spray flame structure and emissions characteristics. The turbulence fluctuation was predicted using k-ε-g and algebraic mixing-length-hypothesis (mlh) turbulence models. The numerical method was evaluated using a set of available experimental data. It is shown that this theoretical model predicts the data well in the near nozzle region and the predictions improve quantitatively along the axial distance. In comparing the turbulence models, the k-ε-g model provides a better result for the varying-density flow of spray combustion.

INTRODUCTION

Spray combustion is widely used in transportation and industrial devices, such as boilers, diesel engines, gas turbines, etc.. However, the complicated phenomena involved in spray combustion such as turbulent two-phase flow, turbulence/chemical kinetic interactions, and finite interphase transport rate retard the development of highly efficient liquid spray combustors. Some theoretical and computer simulation methods have recently been proposed in order to calculate spray flame characteristics. In this study, a theoretical model to predict the combustion phenomena of a steady, axisymmetric turbulent spray is developed. Liquid n-pentane, atomized by the primary air, is assumed to be injected upwards in the combustion chamber. The initial distributions of size, velocity, and direction of liquid drops are formed at the exit of the atomizer. In considering this two-phase problem, the liquid and gas phases are assumed to be in dynamic and thermodynamic equilibria so that they have the same temperature and velocity, implying that the spray combustion may be treated as single-phase gas combustion.

The thermodynamic effects of evaporation and burning on spray flame structure are considered. Prior to oxidation, liquid fuel is vaporized by absorbing the heat diffused from the flame zone. This heat energy is used to raise the liquid temperature to its boiling point. The two-film evaporation model for single-droplet is extended to compute the enthalpy of evaporation of the spray.

Since the rates of mass and heat diffusions are much slower than the rate of reaction in liquid spray combustion, a fast reaction chemical equilibrium is assumed. A computer package code CEC-76 [1], based on the minimization of free energy, along with JANAF [2] thermodynamic data is employed to calculate the concentrations of species, flame temperature, mixture density, molecular weight,... etc. at various mixture fractions. Thus, the state relationships could be constructed under the thermodynamic conditions of constant enthalpies of reactants and products and including of liquid-fuel evaporation. The k-ε-g and algebraic mixing-length-hypothesis (mlh) turbulence models with their corresponding set of empirical constants are employed in the finite difference numerical scheme. These two turbulence models are assessed for their performance and prediction capabilities in the varying-density flow involving spray combustion. Also, the conserved-scalar formulation is assumed in this study so that the scalar properties are related only to mixture fraction and can be determined once the value of mixture fraction is calculated from its finite difference equation.

The Favre-averaged equations are obtained by using a prescribed probability density function. The

shape of the distribution of the pdf is set up by computing the two parameters α and β of the β pdf from the mixture fraction (f) and the concentration fluctuation (g). The Favre-averaged values of temperature, species concentrations, density, ...etc, are thus determined from the integrations by the Simpson's rule method.

EVAPORATION MODEL

The liquid and gaseous phases are mixed homogeneously based on the locally homogeneous flow (LHF) approximation [3]. Liquid fuel is assumed to be completely evaporated prior to the fast chemical reaction. In calculating the enthalpy of evaporation, the thin-film evaporation model of an individual droplet is extended for the local liquid spray. The present model considers the local liquid spray in the flow field as one lump of liquid drops of mass Y_{fu} at one homogeneous liquid temperature, T_l. The exothermic heat release is diffused from the flame zone to the surface of the liquid phase to provide the energy required to raise its initial temperature T_l to the surface temperature, which is assumed as the normal boiling temperature T_b, and the latent heat of evaporation h_{fg}. Hence, the enthalpy of evaporation H_{evap} of liquid fuel to become vapor is given by,

$$H_{evap} = Y_{fu}[C_l(T_b - T_l) + h_{fg}] \quad (1)$$

where C_l is the specific heat of liquid fuel. Y_{fu} in the above equation is obtained from its state relationship with local mixture fraction which is calculated from the finite difference scheme.

COMBUSTION MODEL

In this study, it is intended to investigate whether the combustion model of fast chemical equilibrium is suitable for the spray combustion. The reactant-fuels in these two studies are in different phases. The fundamental difference between the reacting liquids and gases arises because liquids are more continuous than gases in kinetic terms. The molecules in liquids undergo considerably higher frequency of collisions while the molecules in gases travel most of the time between collisions. In other words, the reaction in liquid flow proceeds relatively more rapidly than reactions in gases so that the former is more suitable for the assumption of fast chemistry. Moreover, the density of liquid fuel experiences little variation during reactions, in comparison with the density of gas due to the exothermic effect. This diminishes the influence of chemistry on the velocity field, and the interaction of turbulence and chemical reaction is simplified [4].

Unfortunately, the above simplicities of liquid fuels, are accompanied with the complexities of different magnitudes in the transport properties. In liquids, the order of magnitude of the diffusivity of species is much smaller than those of momentum and heat, while in gases they are of the same order. Consequently, the liquid spray combustion based on the assumption of locally homogeneous flow (LHF) is more suitable for using the approximation of fast chemistry than a gaseous reacting flow if the differences in the orders of magnitude of those diffusivities are neglected.

In this study, it is further assumed that the liquid fuel is suddenly evaporated to the gaseous phase if there is sufficient energy from the flame zone to vaporize the liquid drops, and the vapor immediately reacts with the oxidizer. Thus, the fast chemistry approximation is extended to include that of fast evaporation also. Under these assumptions, the transport properties of heat, species, and momentum may be regarded to be of the same order of magnitude and the combustion model of fast chemistry becomes applicable to the spray combustion study.

EQUATION OF STATE

In this study, the liquid fuel atomized with primary air is assumed to be injected into still air surroundings. Before leaving the atomizer the reactant is composed of both liquid fuel and air. The initial mass fraction of fuel is assumed to be 0.82 in this case, while the mass fraction of the atomizing air is 0.18. Enthalpy and pressure, (H, P) are used to describe the thermodynamic states when employing the CEC-76 package code [1]. This is equivalent to the assumptions of adiabatic flame temperature and invariant pressure field. It should be noted here that the enthalpy of the fuel must be the sum of the enthalpies of vapor and liquid. The heat release from combustion is used up partly for evaporation and partly for increasing the product temperature. The calculations in this code consider dissociations and condensed species. All gases are assumed to be ideal with no phase interactions. The solubility of liquid into air or gaseous species is assumed negligible. The reaction is assumed to occur at any value of mixture fraction while a prescribed Beta density function was utilized to adjust the extent of reaction.

The state-relationships are illustrated in Fig. 1 from which it is seen that the mass fraction of pentane, nitrogen, oxygen, water vapor, hydrogen, carbon dioxide and carbon monoxide are functions of only one independent variable, namely the mixture fraction.

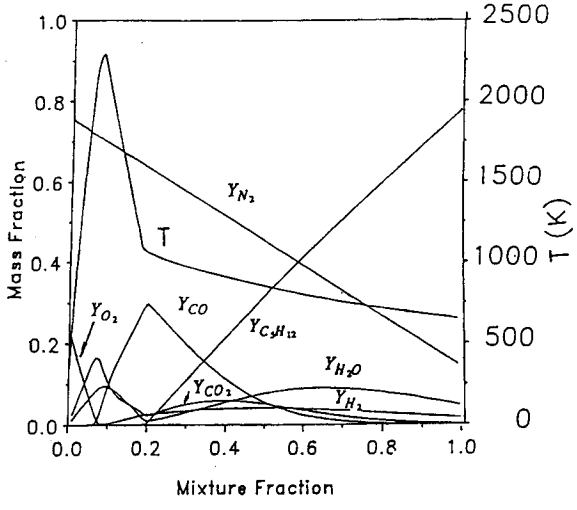

Fig. 1. State Relationship for Pentane Spray Combustion.

PROBABILITY DENSITY FUNCTION

The probability density function was employed in this study to average some combustion properties which are obtained from the mixture fraction so that the influence of turbulence fluctuation on the conserved scalar quantities could be included. The type of probability density function, either a clippsed Gaussian or a beta function, is assumed before the averaging procedure. The beta pdf was employed in the present study due to its simplicity and the associated lower cpu time and cost. The beta pdf is mathematically described by

$$p(f)=\frac{f^{\alpha-1}(1-f)^{\beta-1}}{\int_0^1 f^{\alpha-1}(1-f)^{\beta-1}\,df} \tag{2}$$

where the coefficients α and β are explicit functions of the mass mean mixture fraction ($\tilde{f}$) and concentration fluctuation (g), expressed as

$$\alpha=\tilde{f}\left[\frac{\tilde{f}(1-\tilde{f})}{g}-1\right] \tag{3}$$

$$\beta=(1-\tilde{f})\,\alpha \tag{4}$$

The average values of the species concentration, product temperature, enthalpy, and density are calculated by weighting these quantities with the preassumed probability density functions of mixturefraction, $\tilde{p}(f)$ which could be adequately specified once the $\tilde{f}$ and g are obtained from the finite difference solutions for each grid point. The Favre-averaging quantity Q may be obtained from

$$\tilde{Q}=\int_0^1 \tilde{p}(f)\,Q(f)\,df \tag{5}$$

The quantities of $Y_i(f)$, $H(f)$, $T(f)$ and $\rho(f)$ are the instantaneous functions of mixture fraction (f). After the calculation of α and β from the known values of $\tilde{f}$ and g using Eqns. (3) - (4), the Beta probability density function also depends only on mixture fraction. A suitable number (say N=100) of separate values of $Y_i(f)$, etc., were calculated from the equations of state for mixture fraction in the range of 0 to 1 and stored in tabular form. This procedure simplified the integration of Eqns. (2) - (5) with the Simpson's rule instead of complex integrating procedures.

CALCULATION METHODS

In the present study, the k-ε-g model is used together with Favre-averaging procedure. The Favre-averaged forms of the equations of turbulent kinetic energy (k), turbulent dissipation rate (ε) and concentration fluctuation (g) are used so that the effect of the fluctuation of density could be included in the computation of flow structures and relevant properties. The turbulence effective viscosity μ_t is related to turbulence kinetic energy (k) and turbulence dissipation rate (ε) by $\mu_t=c_\mu\rho k^2/\varepsilon$, in which c_μ is a model constant. The data of k and ε for μ_t were obtained from the calculation of finite difference equations at each grid point of the flow domain derived through partial differential equations describing the behavior of k and ε as follows:

Turbulent kinetic energy equation:

$$\frac{\partial}{\partial x}(\tilde{\rho}\,\tilde{u}\,\tilde{k})+\frac{1}{r}\frac{\partial}{\partial r}(r\,\tilde{\rho}\,\tilde{v}\,\tilde{k})=\frac{1}{r}\frac{\partial}{\partial r}\left[r\left(\mu+\frac{\mu_t}{\sigma_k}\right)\frac{\partial \tilde{k}}{\partial r}\right]$$

$$+\mu_t\left(\frac{\partial \tilde{u}}{\partial r}\right)^2-\tilde{\rho}\,\tilde{\varepsilon} \tag{6}$$

Turbulent dissipation rate equation:

$$\frac{\partial}{\partial x}(\tilde{\rho}\,\tilde{u}\,\tilde{\varepsilon})+\frac{1}{r}\frac{\partial}{\partial r}(r\,\tilde{\rho}\,\tilde{v}\,\tilde{\varepsilon})=\frac{1}{r}\frac{\partial}{\partial r}\left[r\left(\mu+\frac{\mu_t}{\sigma_\varepsilon}\right)\frac{\partial \tilde{\varepsilon}}{\partial r}\right]$$

$$+\left[c_{\varepsilon_1}\mu_t\left(\frac{\partial \tilde{u}}{\partial r}\right)^2-c_{\varepsilon_2}\tilde{\rho}\,\tilde{\varepsilon}\right]\left(\frac{\tilde{\varepsilon}}{\tilde{k}}\right) \tag{7}$$

Concentration fluctuation equation:

$$\frac{\partial}{\partial x}(\tilde{\rho}\,\tilde{u}\,\tilde{g})+\frac{1}{r}\frac{\partial}{\partial r}(r\,\tilde{\rho}\,\tilde{v}\,\tilde{g})=\frac{1}{r}\frac{\partial}{\partial r}\left[r\left(\frac{\mu}{S_c}+\frac{\mu_t}{\sigma_g}\right)\frac{\partial \tilde{g}}{\partial r}\right]$$

$$+c_{g_1}\mu_t\left(\frac{\partial \tilde{f}}{\partial r}\right)^2-c_{g_2}\tilde{\rho}\,\tilde{g}\left](\frac{\tilde{\varepsilon}}{\tilde{k}}\right) \tag{8}$$

It should be noted that tilde ~ and overbar - in the above equations represent mass and time averaged quantities. In the mlh model, the turbulent transport properties are decoupled from the governing partial differential equations of the mean flow. Instead, the length scale of turbulence is computed by means of an algebraic formulation. The effective turbulence viscosity is given by $\mu_t=\rho l^2\left|\frac{\partial u}{\partial r}\right|$, where l=mixing length.

The other Favre-averaged governing equations describing the conservation of mass, momentum, and mixture fraction are given below:

Continuity equation

$$\frac{\partial}{\partial x}(\tilde{\rho}\tilde{u})+\frac{1}{r}\frac{\partial}{\partial r}(r\tilde{\rho}\tilde{v})=0 \tag{9}$$

Momentum equation

$$\frac{\partial}{\partial x}(\tilde{\rho}\tilde{u}\tilde{u})+\frac{1}{r}\left[\frac{\partial}{\partial r}(r\tilde{\rho}\tilde{v}\tilde{u}\frac{\partial u}{\partial r})=\frac{1}{r}\frac{\partial}{\partial r}\left[r(\mu+\mu_t)\frac{\partial u}{\partial r}\right]\right.$$
$$+a(\rho_\infty-\rho) \tag{10}$$

Mixture fraction equation

$$\frac{\partial}{\partial x}(\tilde{\rho}\tilde{u}\tilde{f})+\frac{1}{r}\frac{\partial}{\partial r}(r\tilde{\rho}\tilde{v}\tilde{f})=\frac{1}{r}\frac{\partial}{\partial r}\left[r\left(\frac{\mu}{S_c}\right)+\frac{\mu_t}{\sigma_f}\right)\frac{\partial\tilde{f}}{\partial r}] \tag{11}$$

These governing equations are of parabolic type and therefore can be solved by marching integration [5]. The forward step is limited to a value such that the entrainment is 5% of the total fluid flow of that location.

RESULTS AND DISCUSSIONS

The predictions of spray flame temperature, velocity and mass concentrations of species in the axial and radial directions, as liquid *n*-pentane atomized by the primary air injected into stagnant air, are presented to evaluate the turbulence models of *k-ε-g* and mlh for spray combustion. The experimental data of Szekely [6] are compared with the Favre-averaged properties calculated from the finite-difference equations.

1. Axial Variations of Favre-Averaged Propertiesties

1.1 *Mean Velocity*

The axial centerline velocity normalized by the velocity at the exit of nozzle is shown in Fig.2. The deviations of the predictions of *k-ε-g* and mlh models from the experimental data decrease with the axial distance. The curves of both predictions decline starting from around x/d = 16. The prediction of the *k-ε-g* model shows a more stable and smooth decay of velocity, while that of mlh model varies more abruptly at some points of the flow field. It seems that the mlh model in which turbulence viscosity is obtained from an algebraic formulation gives somewhat worse results in variable-density flows.

In the near-nozzle region, the chemical reactions are not significant because the spray is composed of large drops at low temperature. The mass fractions of the liquid drops and gaseous mixture decrease along the axial direction and the size of the drops approaches a very small value, which is the limiting condition for the validity of the LHF assumption. Hence, the predictions and measurements become closer in the far-nozzle region.

1.2 *Mean Temperature*

The difference of temperatures on the axis and in the air normalized by the initial difference is illustrated in Fig.3. It is seen that the peak temperatures of predictions lie around x/d=100. In the near-nozzle region, the predicted temperature is overestimated and reach the peak earlier since the deviation of the LHF model implying well-atomized drops from the large drop-size is considerable in reality. The predictions are closer to the experimental data beginning from x/d=200.

1.3 *Concentrations Field of Species*

Figure 4 presents the predictions of the mass

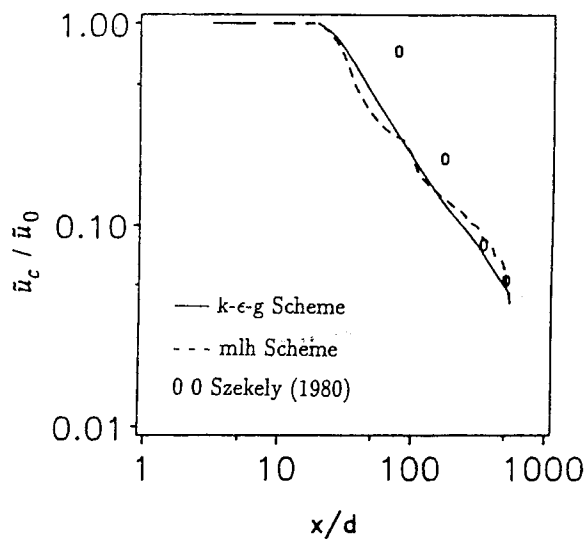

Fig. 2. Axial Variation of Velocity along Central Line.

fractions of species in the axial direction by the k-ε-g scheme. As shown in Fig.4 in the region prior to x/d=80, the mass ratio of fuel/air exceeds the stoichiometric ratio of n-pentane, and the intermediate species CO and H_2 appear. The mass fraction of CO reaches its peak value 0.3 at x/d=80, where pentane is completely depleted and the mass fractions of species CO_2 and H_2O start to rise. As the spray flame extends further to 170 diameters, which corresponds to the reaction region, fuel and oxygen are separated and the peak mass species CO_2 and H_2O occur. The intermediate CO and H_2 disappear from the reaction zone, which represents the location of maximum flame temperature. The flame temperature thereafter decreases as more air is entrained from the surroundings.

1.4 *Mass Fractions of Individual Species*

The comparisons of the mass fractions of the individual combustion species predicted by the k-ε-g and mlh schemes with experimental data are shown in Figs. 5 through 7. The predictions do not seem to agree well with measurements in the near-nozzle region, where the dense spray of large-drops exists so that the combustion reactions are suppressed. However, the differences between predictions and measurements decrease with the increase of axial distance and the agreements become satisfactory around x/d=200, implying that the region of dilute spray conforming to the LHF assumption is approaching.

Figure 5 shows the mass faction of pentane decreasing from 0.81 to 0 at x/d=90 in the predictions of both schemes. The predictions overestimate the mass fraction of pentane. Szekely [6] observed that at x/d=90 the mass fraction of pentane is around 0.3 and decays to 0 at x/d=250, much farther than that predicted. While comparing the k-ε-g and mlh schemes, it is noticed that the latter overestimates this species more than the former.

Figure 6 shows the axial variation of the mass fraction of CO_2. The peak value is predicted to be 0.16 at x/d=180 , which is about two times higher than that found in experiments. The mlh model calculation matches better than that of the k-ε-g model with the data in the far-nozzle region.

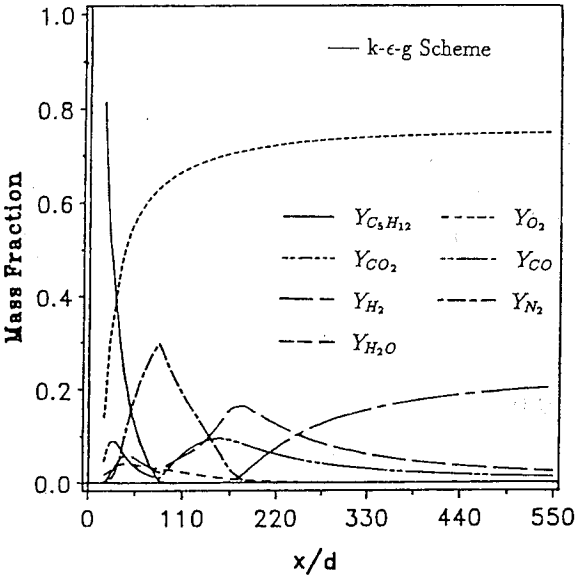

Fig. 4. Axial Variation of Mass Fraction of Species along Central Line.

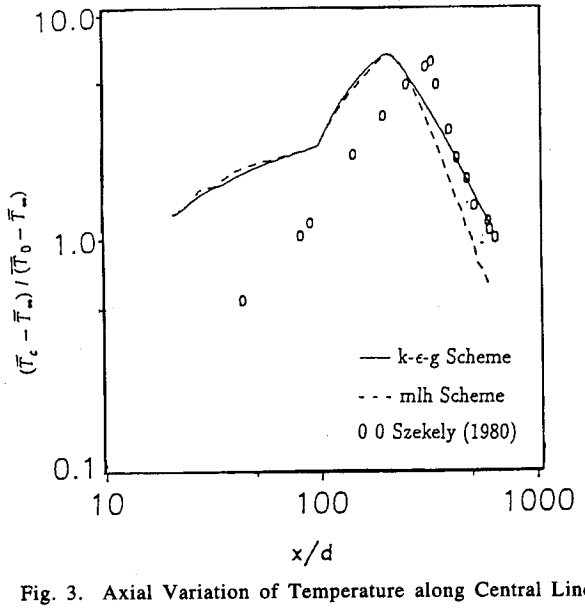

Fig. 3. Axial Variation of Temperature along Central Line.

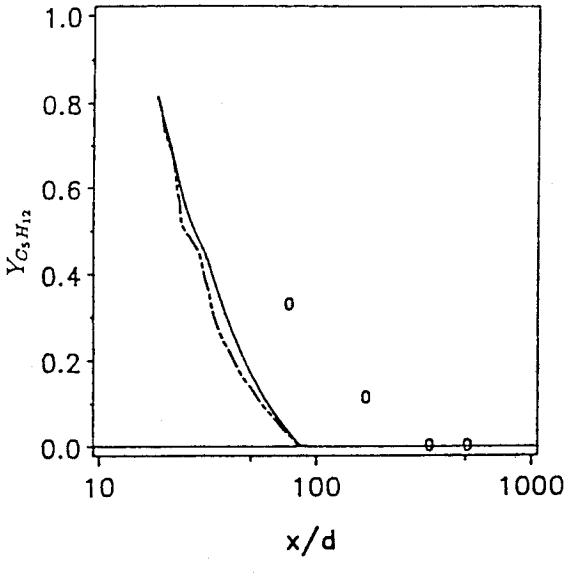

Fig. 5. Axial Variation of Mass Fraction of C5H12 along Central Line.

Figure 7 shows the variation of mass fraction of H_2O along the central axis. The predictions are lower than the data by a factor of about 5. As discussed in section 7.1.2, the combustion process in the models starts about 60 diameters closer to the nozzle-exit than in the experiments. If the predicted curves are pushed forward from the nozzle by 60-diameters, the agreement between predictions and data improves.

2. Radial Variation of Favre-Averaged Properties

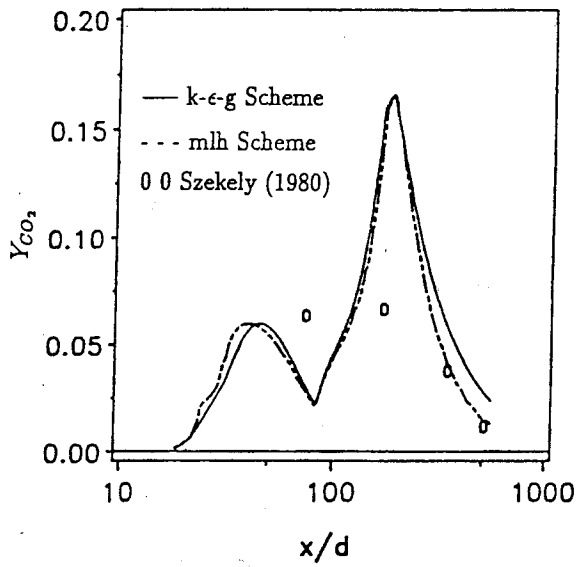

Fig. 6. Axial Variation of Mass Fraction of CO_2 along Central Line.

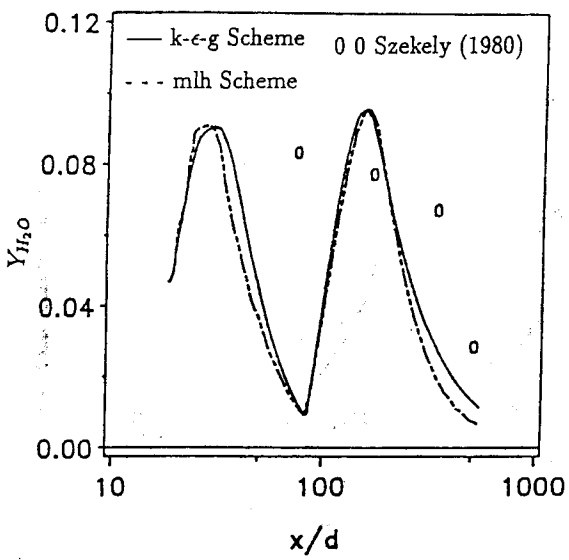

Fig. 7. Axial Variation of Mass Fraction of H2O along Central Line.

2.1 *Mean Velocity*

The variation of the axial velocity along the radial direction at three axial positions x/d = 170, 340 and 510 is shown in Fig.8. The predictions of the k-ε-g and mlh models are compared with the available experimental data. It is shown that k-ε-g model predicts a farther jet spread than that by mlh model. Also, the results of the k-ε-g model agree with the experimental data better at these three axial distances.

2.2 *Mean Temperature*

In Fig.9, the predicted difference of temperature at the radial location and in the surrounding air normalized by the temperature difference between the axis and the surrounding air are compared with measurement. The mlh model provides higher predictions at all three axial distances, but the curves of k-ε-g model extend longer. Over most of the flow field, the predictions of the mlh model agrees well with the data, especially the peak temperature around r/x = 0.07 at x/d = 170. In general, both predictions are satisfactory at x/d = 340 and 510, but they overestimate the temperature near the edge of the spray at x/d = 170.

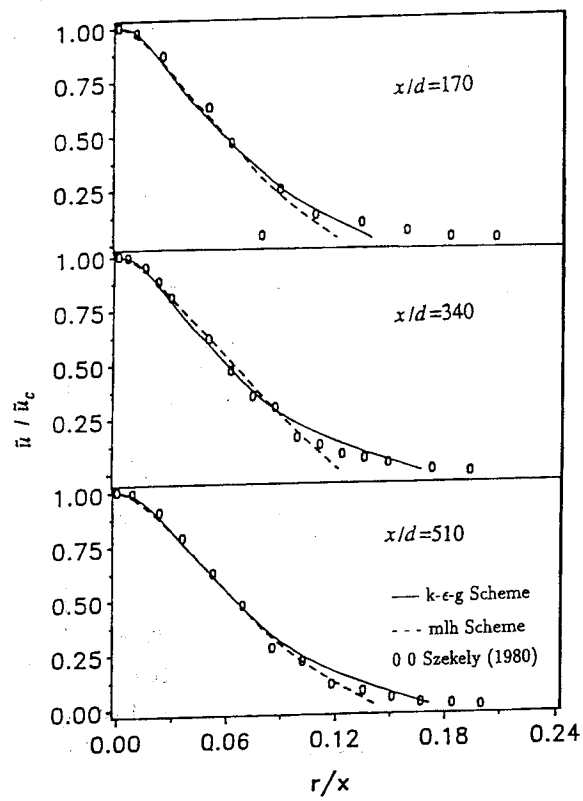

Fig. 8. Radial Variation of Velocity for Pentne Spray Combustion.

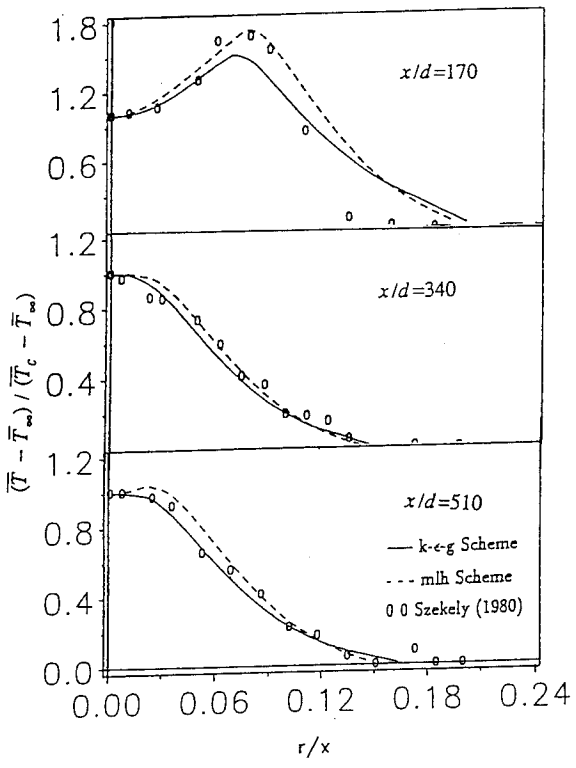

Fig. 9. Radial Variation of Temperature for Pentane Spray Combustion

CONCLUSIONS

A theoretical model for liquid spray combustion atomized by primary air in an axisymmetric domain was developed and evaluated. Results of the numerical calculations by the k-ε-g and mlh turbulence models are compared with the available experimental data of the profiles of the velocity, temperature, and mass fractions of species in the axial and radial directions. This study shows that the predictions of theoretical models improve along the axial distance. The predictions of velocity, temperature and species mass fractions in the near-nozzle region are worse mainly due to the high liquid to gas mass ratio. In comparing the k-ε-g and mlh models, it is generally noticed that their predictions are close enough. However, the former provides a smoother description of the phenomena involved. It seems as though that the k-ε-g model is more suitable for predicting varying-density flows such as the spray flame of this study.

NOMENCLATURE

d = Injector diameter
f = Mixture fraction
g = Concentration fluctuation
H = Enthalpy
κ = Turbulence kinetic energy
T = Flame temperature
r = Radial distance
u = Axial velocity
v = Radial velocity
x = Axial distance
Y = Mass fraction
ε = Turbulence dissipation rate
μ = Laminar viscosity
μ_t = Turbulent viscosity
ρ = Density

Superscripts

$\sim$ = Mass-averaged
$-$ = Time-averaged

Subscripts

b = Boiling point
c = Axial centerline of spray
fu = Fuel
l = Liquid
0 = Exit of nozzle
∞ = Ambience

REFERENCES

1. Gordon, S. and McBride, B.J., *Computer Pro gram for Calculation Complex Chemical Equilbrium Composition, Rocket Performance, Incident and Reflected Shocks, and Chapman-Jouguet Detonations.* NASA Lewis Research Center (1976).
2. Anon, *JANAF Thermodynamics Tables.* Dow Chemical Co., Midland, Michigan (1970).
3. Faeth, G.M.," Mixing, Transport and Combustion in Sprays." *Prog. Energy Combust. Sci.* Vol. 13, pp. 293-345 (1987).
4. Libby, P.A. and Williams, F.A., "Fundamental As pects." *Topics in Applied Physics- Turbulent Reacting Flows (1980).* Spring-Verlag, pp. 1-43.
5. Anderson, D.A., Tannehill, J.C. and Pletcher, R.H., *Computational Fluid Mechanics and Heat Transfer.* Hemisphere Publishing Co. (1984).
6. Szekely, G.A., Jr., *Experimental Evaluation of a Locally Homogeneous Flow Model of Spray Combustion.* M.S. Thesis, The Pennsylvania State University, University Park, PA. (1980).